



**Ministry of Hight Education
and Scientific Research
University of Diyala
College of Science
Department of physics**



Synthesis of Magnetic Nanoparticles for Water Treatment Applications

A Thesis

Submitted to the College of Science, University of Diyala in
Partial Fulfillment of the Requirements for the Degree of Doctor of
philosophy in physics.

By

Basem Abd. Ibrahim

B.Sc.1999

M.Sc. 2016

Supervised by

Prof. Dr. Tahseen H. Mubarak

Prof. Dr. Abdul Mun'em A.Karim

2022 A.D

1444 A.

بِسْمِ اللَّهِ الرَّحْمَنِ الرَّحِيمِ

قالوا سبحانك لا علم لنا إلا ما علمتنا

إنهم ذنوب العليم والحكيم

صدق الله العظيم

البقرة الآية (٣٢)

DEDICATIONS

I dedicate this study with much Gratitude and Love;

To the pure soul, my father, I ask Allah to have mercy on him and make his grave a meadow from the gardens of Paradise and gather me with him in Paradise.

For her Love, endless support, and encouragement my mother.

Who have shared my success and supported me to make my dream come true my wife and children.

The giving and support symbol my brothers and sisters.

To the kind hearts, to the lovely people with whom I spent the most precious moments in my life, my teachers.

Basem

ACKNOWLEDGMENTS

First of all, I thank Almighty Allah who has enabled me to continue this work and overcome all difficulties. I would like to express my sincere gratitude to my supervisors Prof. Dr. Tahseen H. Mubarak, and Prof. Dr. Abdul Mun'em A. Karim for their encouragement, guidance, and scientific support throughout this study.

I would like to express my appreciation to Dr. Omar Ahmad Hussein for helping me . Prof .Dr Ahmed Najem Abd. and college of science department of physics.

Basem

Abstract

In this study magnetic nanoparticles were prepared in two forms, the first is $\text{Ni}_{1-x}\text{Co}_x\text{Fe}_2\text{O}_4$ and the second is $\text{Ni}_{1-x}\text{Mg}_x\text{Fe}_2\text{O}_4$ for the x values, (x= 0.0,0.1,0.3,0.5,0.7) respectively by chemical co-precipitation thermal method and annealed at temperature of (700 °C) and pH=11.

The structural properties of the prepared samples were studied by using the energy-dispersive X-ray spectroscopy EDX, the scanning electron microscope, the XRD spectroscopy, and the Fourier transforms Infra-red of the FT-IR infrared spectrometer. The synthetic results showed that the prepared particles possess practical proportions that correspond largely to the theoretical proportions, which means the validity of the proposed structures and all the samples show nearly perfect stoichiometry and high purity. This is what is observed from the EDX measurements. The SEM analysis reveals the increasing proportion of cobalt and magnesium for both compounds, and that the particles had spherical and irregular geometric structures within sizes that were often greater than 100 nm. The powder XRD pattern confirms a single-phase cubic spinel structure and the average particle size calculated via the Scherrer equation ranged between (16.31-29.53) nm. Based on X-ray diffraction, information were very close to those recorded using microscopy SEM, and the FTIR spectra confirmed two peaks (ν_1 and ν_2) around 400 and 600 cm^{-1} , respectively. These bands are attributed to the stretching vibration of interactions between the oxygen atom and the cations in tetrahedral and octahedral sites. Therefore, bands indicate that the spectral composition of all samples is ferrite.

The magnetic properties of the particles through the VSM test showed that the addition of cobalt and magnesium to the NiFe_2O_4 was improved the magnetic properties of the main ferrite with a good to high ratio from the narrowness of the hysteresis loop give the characteristics of a soft ferrite.

The work presented in this thesis focused on the efficient use of magnetic nanoparticles in water treatment processes. It involves choosing the best two samples of prepared magnetic nanoparticles from each mixture based on their structural and magnetic properties for use in the removal of lead and cadmium ions from aqueous solution under laboratory conditions. The GO- 2(N-morpholino ethanesulfonic acid) was used to prepare novel magnetic adsorbents by mixing with the best four ferrites. Among these four nanoparticles are com.1 (GO- 2(N-morpholinoethanesulfonic acid)- $\text{Ni}_{0.9}\text{Co}_{0.1}\text{Fe}_2\text{O}_4$), com.2 (GO- 2(N-morpholinoethanesulfonic acid)- $\text{Ni}_{0.5}\text{Co}_{0.5}\text{Fe}_2\text{O}_4$), com.3 (GO-2(N-morpholinoethanesulfonic acid)- $\text{Ni}_{0.7}\text{Mg}_{0.3}\text{Fe}_2\text{O}_4$), and Com.4 (GO-2(N-morpholinoethanesulfonic acid)- $\text{Ni}_{0.5}\text{Mg}_{0.5}\text{Fe}_2\text{O}_4$).

After determining the optimal concentration of lead and cadmium, The following optimal conditions were studied: contact time, adsorbent quantity, acidity, and temperature. The optimal concentration was (100 ppm) for all conditions except composite 4, where the removal of lead ions was (250 ppm).

Through the experiments, it was observed that with an increase in the contact time, pH, the dosage, and temperature, the percentage of removal of lead and cadmium ions increased from the aqueous solution. Among the four magnetic nanoparticles, results showed that the (com2) and (com4). gave the best percentage of removal of lead and cadmium ions from the aqueous

solution. The kinetic results of adsorption showed that the adsorption of lead and cadmium ions by the magnetic nanoparticles surfaces followed a pseudo-second order equation based on the values of (R^2) and from studying the isotherms of Freundlich, Langmuir, and Temkin models of the four compounds. The results show the Freundlich isotherm is the ruling isotherm in these materials, as it was perfectly suitable for all adsorption cases despite the relatively few differences with the (R^2) values for the rest of the isotherms. This confirms that the adsorption was of a heterogeneous type. The approaches and treatment methods described in this thesis are simple to use, robust and environmental friendly.

List of Contents

No.	Subject	Page
	DEDICATIONS	I
	ACKNOWLEDGMENT	II
	Abstract	III
	List of Contents	VI
	List of Figures	XIII
	List of Tables	XX
	List of Symbols	XXI
Chapter One (Introduction and Previous Studies)		
1.1	Introduction	1
1.2	History of Magnetic Materials	1
1.3	Ferrites	2
1.4	Synthesis of Ferrite Nanoparticles	2
1.5	Nanotechnology and Nanomaterials	3
1.5.1	Classification of Nanomaterials	4
1.5.2	Production Methods of Nanomaterials	5
1.6	Applications of Ferrites	6
1.7	Previous Studies	9
1.8	Study Aim	16
Chapter Two (Theoretical Part)		
2.1	Introduction	17

2.2	Fundamentals of Magnetism and Magnetic Materials	17
2.2.1	The Origin of Magnetism	17
2.2.2	Magnetic Field and Magnetic Influence	18
2.3	Classification of Magnetic Materials	19
2.3.1	Diamagnetic Materials	19
2.3.2	Paramagnetic Materials	20
2.3.3	Ferromagnetic Materials	21
2.3.4	Antiferromagnetic Materials	23
2.3.5	Ferrimagnetic Materials	24
2.4	The Ferrites	25
2.4.1	Hexagonal Ferrites	25
2.4.2	Garnet Ferrites	25
2.4.3	Spinel Ferrites	26
2.5	Nano-Ferrites	28
2.6	Nickel Ferrites	29
2.7	Magnetic Hysteresis (M-H) Loop	30
2.7.1	Types of Ferrites	31
2.8	Water Treatment Study	32
2.8.1	Water Pollution	32
2.8.2	Effects of Water Pollution	33
2.8.3	Classification of Water Pollutants	33
2.9	Heavy Metals and Its Effects on Environment	34
2.10	Magnetic Nanoparticles	35
2.11	Use of Magnetic Nanoparticles as Adsorbent Surface	36
2.12	Nanotechnology in Wastewater Treatment	37
2.12.1	Adsorption	37
2.12.1.1	Types of Adsorption	38
2.12.1.2	Factors Affecting the Adsorption Process	39

2.13	Adsorption Kinetics	40
2.13.1	First Order Model	41
2.13.2	Second Order Model	41
2.14	Adsorption Isotherms	42
2.14.1	Theory of Adsorption	43
2.14.1.1	Langmuir Isotherm	43
2.14.1.2	Freundlich Isotherm	44
2.14.1.3	Temkin Isotherm	45
2.15	The Characterization Techniques	46
2.15.1	X-Ray Diffraction Technology (XRD)	47
2.15.2	Scanning Electron Microscopy (SEM)	48
2.15.3	Fourier Transformation Infrared Spectroscopy (FTIR)	49
2.15.4	Energy-Dispersive X-Ray Spectroscopy (EDX)	50
2.15.5	Vibrating Sample Magnetometer (VSM)	50
2.15.6	Transmission Electron Microscopy (TEM)	52
2.15.7	Atomic Absorption Spectrophotometers (AAS)	52
Chapter Three (Experimental Part)		
3.1	Introduction	54
3.2	Chemical Materials	54
3.3	Instruments	55
3.3.1	Sensitive Electronic Balance	55
3.3.2	Magnetic Stirrer	55
3.3.3	pH meter	55
3.3.4	Furnace	55
3.3.5	Ultra –Sonic Water Bath	56
3.4	Synthesis Techniques of Nanoparticles	56

3.4.1	Sol-Gel Method	56
3.4.2	Chemical Co- Precipitation Method	57
3.5	Synthesis of Ferrite Nanoparticles	57
3.5.1	Synthesis of (Ni-CoFe ₂ O ₄)	57
3.5.1.1	Calculation of the Molecular Weights of Substances	57
3.5.1.2	Calculating the Weight of the Materials Used in the Preparation of Magnetic Nanoparticles	58
3.5.1.3	Method of Prepared	59
3.5.2	Synthesis of (Ni-MgFe ₂ O ₄)	63
3.5.2.1	Calculation of the Molecular Weights of Substances	63
3.5.2.2	Calculating the Weight of the Materials Used in the Preparation of Magnetic Nanoparticles	63
3.5.2.3	Method of Prepared	64
3.6	Thermal Treatment	69
3.7	Structure Characterization	69
3.7.1	X-Ray Diffraction Measurement (XRD)	69
3.7.2	Scanning Electron Microscopy (SEM)	70
3.7.3	Energy-Dispersive X-Ray Spectroscopy (EDX)	70
3.7.4	Fourier Transform Infrared Spectroscopy (FT-IR)	71
3.8	Magnetic Measurement	71
3.9	Synthesis of Graphene Oxide By Hummers Method	71
3.10	Synthesis of Graphene Oxide-Derivative (GO- 2(N-morpholinoethansulfonic acid)	72
3.11	Working Mechanism	73
Chapter Four (Results and Discussion)		
4.1	Synthesis and Characterization of Ferrites	74
4.1.1	Synthesis	74
4.2	Characterization	75

4.2.1	XRD Measurement	75
4.2.2	EDX Measurement	78
4.2.2.1	EDX Analyze of NiFe ₂ O ₄	79
4.2.2.2	EDX Analyze of Ni _{0.9} Co _{0.1} Fe ₂ O ₄	80
4.2.2.3	EDX Analyze of Ni _{0.7} Co _{0.3} Fe ₂ O ₄	80
4.2.2.4	EDX Analyze of Ni _{0.5} Co _{0.5} Fe ₂ O ₄	81
4.2.2.5	EDX Analyze of Ni _{0.3} Co _{0.7} Fe ₂ O ₄	82
4.2.2.6	EDX Analyze of Ni _{0.9} Mg _{0.1} Fe ₂ O ₄	84
4.2.2.7	EDX Analyze of Ni _{0.7} Mg _{0.3} Fe ₂ O ₄	84
4.2.2.8	EDX Analyze of Ni _{0.5} Mg _{0.5} Fe ₂ O ₄	85
4.2.2.9	EDX Analyze of Ni _{0.3} Mg _{0.7} Fe ₂ O ₄	86
4.2.3	SEM Measurement	86
4.2.3.1	SEM Analyze of NiFe ₂ O ₄	86
4.2.3.2	SEM Analyze of Ni _{0.9} Co _{0.1} Fe ₂ O ₄	87
4.2.3.3	SEM Analyze of Ni _{0.7} Co _{0.3} Fe ₂ O ₄	88
4.2.3.4	SEM Analyze of Ni _{0.5} Co _{0.5} Fe ₂ O ₄	89
4.2.3.5	SEM Analyze of Ni _{0.3} Co _{0.7} Fe ₂ O ₄	90
4.2.3.6	SEM Analyze of Ni _{0.9} Mg _{0.1} Fe ₂ O ₄	91
4.2.3.7	SEM Analyze of Ni _{0.7} Mg _{0.3} Fe ₂ O ₄	91
4.2.3.8	SEM Analyze of Ni _{0.5} Mg _{0.5} Fe ₂ O ₄	92
4.2.3.9	SEM Analyze of Ni _{0.3} Mg _{0.7} Fe ₂ O ₄	92
4.2.4	FT-IR Measurement	94

4.2.5	Vibrating-Sample Magnetometer (VSM)	99
4.2.6	Synthesis and Characterization of (GO- 2(N-morpholinoethansulfonic acid)	102
4.2.6.1	Synthesis and Characterization of Graphene Oxide	102
4.2.6.1.1	FTIR of Graphene Oxide	103
4.2.6.1.2	¹ H-NMR Spectrum of Graphene Oxide	103
4.2.6.1.3	XRD Pattern of Graphene Oxide	104
4.2.6.1.4	SEM of Graphene Oxide	105
4.2.6.2.	Characterization of GO-2(N-morpholinoethansulfonic acid)	106
4.2.6.2.1	FTIR of GO- 2(N-morpholinoethansulfonic acid)	106
4.2.6.2.2	¹ H-NMR of GO - 2(N-morpholinoethansulfonic acid)	107
4.2.6.2.3	XRD of GO- 2(N-morpholinoethansulfonic acid)	108
4.2.6.2.4	TEM of GO- 2(N- morpholinoethansulfonic acid)	109
4.2.7	Synthesis and characterization of (GO-2(N-morpholinoethansulfonic acid)-Ferrites	110
4.2.7.1	XRD of Preparing GO-2(N-morpholinoethansulfonic acid)-Ferrites	110
4.2.7.2	VSM of Preparing GO-2(N-morpholinoethansulfonic acid)-Ferrites	113
4.2.7.3	TEM of Preparing GO-2(N-morpholinoethansulfonic acid)-Ferrites	115
4.8	Water Treatment Applications	117
4.8.1	Optimization Studies	117
4.8.1.1	Optimal Conditions for the Adsorption of Lead ions	118
4.8.1.2	Optimal Conditions for the Adsorption of Cadmium ions	122

4.9	Adsorption kinetics study	125
4.9.1	Pseudo First Order Model	125
4.9.2	Pseudo Second Order Model	130
4.10	Isotherms Study	135
4.11	Mechanism of Adsorption	148
Chapter Five (Conclusions and Future Studies)		
5.1	Conclusions	150
5.2	Future Studies	153
	References	154

List of Figures

No.	Subject	Page
Chapter One (Introduction and Previous Studies)		
1.1	Schematic draw of bottom-up and top-down approach	6
Chapter Two (Theoretical Part)		
2.1	Demonstrating the movement of the electron around the nucleus	18
2.2	Demonstrating what happens in a diamagnetic material before, and after an external magnetic field is applied	20
2.3	Demonstrating what happens in a paramagnetic material before, and after an external magnetic field is applied	21
2.4	Demonstrating what happens in a ferromagnetic material before, and after an external magnetic field is applied	22
2.5	Demonstrating what happens in an antiferromagnetic material before, and after an external magnetic field is applied	23
2.6	Demonstrating what happens in a ferrimagnetic material before, and after an external magnetic field is applied	24
2.7	The crystal structure of a spinel shows actions at tetrahedral and octahedral sites	26
2.8	Increases of the surface area with particle size decreases	28
2.9	The classical physics and quantum physics	29
2.10	Magnetization (M) versus magnetic field strength (H)	31
2.11	Demonstrating the difference between physical and chemical adsorption	38

2.12	Giles classification adsorption isotherm	43
2.13	Schematic diagram of X-ray diffraction	48
2.14	The photograph of experimental setup of vibrating sample magnetometer	51
Chapter Three (Experimental Part)		
3.1	The stages of preparation three solutions	59
3.2	The stage of mixing solutions and obtaining a homogeneous solution	60
3.3	The stage of distillation on the mixture	60
3.4	Indicates the heating stage of the mixture	61
3.5	It shows the stage of washing the precipitate and obtaining the powder	61
3.6	Schematic diagram showing the method of preparing (Ni-CoFe ₂ O ₄) by the chemical co-precipitation thermal method	62
3.7	The stages of preparation three solutions	65
3.8	The stage of mixing solutions and obtaining a homogeneous solution	65
3.9	The stage of distillation on the mixture	66
3.10	Indicates the heating stage of the mixture	66
3.11	It shows the stage of washing the precipitate and obtaining the powder	67
3.12	Schematic diagram showing the method of preparing (Ni-MgFe ₂ O ₄) by the chemical co-precipitation thermal method	68
3.13	Shows calcination, for samples of the two compounds (Ni-CoFe ₂ O ₄ and Ni-MgFe ₂ O ₄)	69

3.14	The stages of preparation of graphene oxide	72
3.15	The experimental setup as an example for heavy metals removal from water	73
Chapter Four (Results and Discussion)		
4.1	XRD of $Ni_{1-x}Co_x Fe_2O_4$	75
4.2	XRD of $Ni_{1-x}Mg_xFe_2O_4$	76
4.3	EDX analysis of $NiFe_2O_4$	79
4.4	EDX analysis of $Ni_{0.9}Co_{0.1}Fe_2O_4$	80
4.5	EDX analysis of $Ni_{0.7}Co_{0.3}Fe_2O_4$	81
4.6	EDX analysis of $Ni_{0.5}Co_{0.5}Fe_2O_4$	81
4.7	EDX analysis of $Ni_{0.3}Co_{0.7}Fe_2O_4$	82
4.8	EDX analysis of $Ni_{0.9}Mg_{0.1}Fe_2O_4$	84
4.9	EDX analysis of $Ni_{0.7}Mg_{0.3}Fe_2O_4$	85
4.10	EDX analysis of $Ni_{0.5}Mg_{0.5}Fe_2O_4$	85
4.11	EDX analysis of $Ni_{0.3}Mg_{0.7}Fe_2O_4$	86
4.12	SEM analysis of $NiFe_2O_4$	87
4.13	SEM analysis of $Ni_{0.9}Co_{0.1}Fe_2O_4$	87
4.14	SEM analysis of $Ni_{0.7}Co_{0.3}Fe_2O_4$	89
4.15	SEM analysis of $Ni_{0.5}Co_{0.5}Fe_2O_4$	89
4.16	SEM analysis of $Ni_{0.3}Co_{0.7}Fe_2O_4$	90
4.17	SEM analysis of $Ni_{0.9}Mg_{0.1}Fe_2O_4$	91
4.18	SEM analysis of $Ni_{0.7}Mg_{0.3}Fe_2O_4$	92
4.19	SEM analysis of $Ni_{0.5}Mg_{0.5}Fe_2O_4$	92

4.20	SEM analysis of $\text{Ni}_{0.3}\text{Mg}_{0.7}\text{Fe}_2\text{O}_4$	93
4.21	FTIR of NiFe_2O_4	95
4.22	FTIR of $\text{Ni}_{0.9}\text{Co}_{0.1}\text{Fe}_2\text{O}_4$	95
4.23	FTIR of $\text{Ni}_{0.7}\text{Co}_{0.3}\text{Fe}_2\text{O}_4$	96
4.24	FTIR of $\text{Ni}_{0.5}\text{Co}_{0.5}\text{Fe}_2\text{O}_4$	96
4.25	FTIR of $\text{Ni}_{0.3}\text{Co}_{0.7}\text{Fe}_2\text{O}_4$	97
4.26	FTIR of $\text{Ni}_{0.9}\text{Mg}_{0.1}\text{Fe}_2\text{O}_4$	97
4.27	FTIR of $\text{Ni}_{0.7}\text{Mg}_{0.3}\text{Fe}_2\text{O}_4$	98
4.28	FTIR of $\text{Ni}_{0.5}\text{Mg}_{0.5}\text{Fe}_2\text{O}_4$	98
4.29	FTIR of $\text{Ni}_{0.3}\text{Mg}_{0.7}\text{Fe}_2\text{O}_4$	99
4.30	VSM diagram of $\text{Ni}_{1-x}\text{Co}_x\text{Fe}_2\text{O}_4$	100
4.31	VSM diagram of $\text{Ni}_{1-x}\text{Mg}_x\text{Fe}_2\text{O}_4$	100
4.32	Schematic diagram showing the method of preparing graphene oxide	102
4.33	FTIR spectrum of graphene oxide	103
4.34	$^1\text{H-NMR}$ spectrum of graphene oxide	104
4.35	XRD of graphene oxide	105
4.36	SEM of graphene oxide	105
4.37	Schematic diagram showing the method of preparing GO-2(N-morpholinoethansulfonic acid)	106
4.38	FTIR spectrum of GO-sulfonic acid	107
4.39	$^1\text{H-NMR}$ of GO- 2(N-morpholinoethansulfonic acid)	108
4.40	XRD of GO-2(N-morpholinoethan sulfonic acid)	109
4.41	TEM of GO-2(N-morpholinoethan sulfonic acid)	109

4.42	Schematic diagram showing the method of preparing GO-2(N-morpholinoethansulfonic acid)-ferrites	110
4.43	XRD of GO- 2(N-morpholinoethansulfonic acid)- Ni _{0.9} Co _{0.1} Fe ₂ O ₄	111
4.44	XRD of GO- 2(N-morpholinoethansulfonic acid)- Ni _{0.5} Co _{0.5} Fe ₂ O ₄	111
4.45	XRD of GO- 2(N-morpholinoethansulfonic acid)- Ni _{0.7} Mg _{0.3} Fe ₂ O ₄	112
4.46	XRD of GO- 2(N-morpholinoethansulfonic acid)- Ni _{0.5} Mg _{0.5} Fe ₂ O ₄	112
4.47	VSM of GO- 2(N-morpholinoethansulfonic acid)- Ni _{0.9} Co _{0.1} Fe ₂ O ₄	113
4.48	VSM of GO- 2(N-morpholinoethansulfonic acid)- Ni _{0.5} Co _{0.5} Fe ₂ O ₄	114
4.49	VSM of GO- 2(N-morpholinoethansulfonic acid)- Ni _{0.7} Mg _{0.3} Fe ₂ O ₄	114
4.50	VSM of GO- 2(N-morpholinoethansulfonic acid)- Ni _{0.5} Mg _{0.5} Fe ₂ O ₄	115
4.51	TEM of GO- 2(N-morpholinoethansulfonic acid)- Ni _{0.9} Co _{0.1} Fe ₂ O ₄	115
4.52	TEM of GO- 2(N-morpholinoethansulfonic acid)- Ni _{0.5} Co _{0.5} Fe ₂ O ₄	116
4.53	TEM of GO-2(N-morpholinoethansulfonic acid)- Ni _{0.7} Mg _{0.3} Fe ₂ O ₄	116
4.54	TEM of GO-2(N-morpholinoethansulfonic acid)- Ni _{0.5} Mg _{0.5} Fe ₂ O ₄	117
4.55	The effect of contact time on the adsorption of lead ion	119
4.56	The effect of pH on the adsorption of lead ion	120
4.57	The effect of dosage on the adsorption of lead ion	121
4.58	The effect of temperature on the adsorption of lead ion	122
4.59	The effect of contact time on the adsorption of cadmium ion	122
4.60	The effect of pH on the adsorption of cadmium ion	123
4.61	The effect of dosage on the adsorption of cadmium ion	123
4.62	The effect of temperature on the adsorption of cadmium ion	124

4.63	First order of Pb(II) in composite 1	127
4.64	First order of Pb(II) in composite 2	127
4.65	First order of Pb(II) in composite 3	128
4.66	First order of Pb(II) in composite 4	128
4.67	First order of Cd(II) composite 1	128
4.68	First order of Cd(II) composite 2	129
4.69	First order of Cd(II) composite 3	129
4.70	First order of Cd(II) composite 4	129
4.71	Second order of Pb(II) composite 1	130
4.72	Second order of Pb(II) composite 2	130
4.73	Second order of Pb(II) composite 3	131
4.74	Second order of Pb(II) composite 4	131
4.75	Second order of Cd(II) composite 1	131
4.76	Second order of Cd(II) composite 2	132
4.77	Second order of Cd(II) composite 3	132
4.78	Second order of Cd(II) composite 4	132
4.79	Langmuir isotherm of Pb(II) compound 1	138
4.80	Langmuir isotherm of Pb(II) compound 2	138
4.81	Langmuir isotherm of Pb(II) compound 3	139
4.82	Langmuir isotherm of Pb(II) compound 4	139
4.83	Langmuir isotherm of Cd(II) compound 1	139
4.84	Langmuir isotherm of Cd(II) compound 2	140

4.85	Langmuir isotherm of Cd(II) compound 3	140
4.86	Langmuir isotherm of Cd(II) compound 4	140
4.87	Freundlich isotherm of Pb(II) compound 1	141
4.88	Freundlich isotherm of Pb(II) compound 2	141
4.89	Freundlich isotherm of Pb(II) compound 3	141
4.90	Freundlich isotherm of Pb(II) compound 4	142
4.91	Freundlich isotherm of Cd(II) compound 1	142
4.92	Freundlich isotherm of Cd(II) compound 2	142
4.93	Freundlich isotherm of Cd(II) compound 3	143
4.94	Freundlich isotherm of Cd(II) compound 4	143
4.95	Temkin isotherm of Pb(II) compound 1	143
4.96	Temkin isotherm of Pb(II) compound 2	144
4.97	Temkin isotherm of Pb(II) compound 3	144
4.98	Temkin isotherm of Pb(II) compound 4	144
4.99	Temkin isotherm of Cd(II) compound 1	145
4.100	Temkin isotherm of Cd(II) compound 2	145
4.101	Temkin isotherm of Cd(II) compound 3	145
4.102	Temkin isotherm of Cd(II) compound 4	146
4.103	Scheme proposed mechanism of adsorption	149

List of Tables

No.	Subject	Page
2.1	Lead and cadmium adsorption of synthesized materials	46
3.1	The physical and chemical properties for compounds	54
3.2	The weights of the materials used in the preparation of (Nickel-Cobalt Ferrite)	58
3.3	The weights of the materials used in the preparation of (Nickel-Magnesium Ferrite)	64
4.1	XRD information with Miller indices and average particle size of prepared compounds	76
4.2	The synthesized ferrites and the EDX results	83
4.3	SEM results	88
4.4	It shows the values of saturation magnetization (M_s) and residual magnetization (M_r) for each of the two compounds at a temperature 700 °C	101
4.5	XRD data of graphene oxide	104
4.6	The optimum conditions for the Pb(II)	124
4.7	The optimum conditions for the Cd(II)	125
4.8	Pseudo first order and Pseudo second order	134
4.9	Langmuir, Freundlich and Temkin data	147

List of Symbols

Symbol	Definition
XRD	X-Ray Diffraction (XRD)
SEM	Scanning Electron Microscopy(SEM)
FTIR	Fourier Transformation Infrared Spectroscopy(FTIR)
EDX	Energy-Dispersive X-Ray spectroscopy(EDX)
VSM	Vibrating Sample Magnetometer(VSM)
TEM	Transmission Electron Microscopy(TEM)
AAS	Atomic Absorption Spectrophotometers(AAS)
χ	Magnetic susceptibility
H	Magnetic field
M	Magnetization
λ	Constant of proportionality
μ	Permeability of medium
μ_0	Permeability of space
χ_m	Molar magnetic susceptibility
q_e	The adsorption amount at equilibrium (mg/g)
C_e	The equilibrium concentration of adsorbate in solution (mg/L)
t	The contact time (min)
K_F	Freundlich constant
n	Adsorption intensity

q_{\max}	The theoretical adsorption capacity at equilibrium time (mg/g)
K_L	Langmuir isotherm constant (L/mg)
T	The absolute temperature (K)
R	The gas constant (8.314 KJ/mol.k)
K_T	The binding equilibrium binding constant (L/mg)
b_T	Temkin isotherm constant
B_T	The constant related to heat of sorption (J/ molL)
q_t	The adsorption amount at the time (mg/g)
K_1	The adsorption velocity rate constant of the first order (min^{-1})
K_2	The adsorption velocity rate constant of the second order ($\text{g.mg}^{-1}.\text{min}^{-1}$)
D	The crystallites size(nm)
β	The peaks full width at half maximum(FWHM)
N	The number Avogadro(6.022×10^{23})
M'	The molar concentration
m	The weight (g)
GO	Graphene Oxide

Chapter One
(Introduction and Previous Studies)

1.1. Introduction

This chapter deals an introduction to magnetism materials, applications of ferrites, previous studies, and study aim.

1.2. History of Magnetic Materials

Recently, magnetic materials can be used in many products, such as electronic apparatuses, data processing apparatuses, and communication instruments. These materials have become part of our lives. The magnetic materials that were used in the first applications are metallic magnets, but for frequencies above MHz, metals and alloys do not fit soft magnets, since eddy current losses are very large. According to the work of George J. Orenchak, soft ferrite is a magnetic material used primarily as a core of high-frequency inductors and transformers. Ferrite has gained attention because it attracts iron. The magnetite was found in magnesia district located in the Asia Minor and therefore, named magnetite. In 1909 Hilpert tried to improvise the magnetic properties magnetic materials lead to better results in obtaining high-frequency materials known as ferrites [1].

As a result of their electrical and magnetic characteristics, ferrites are useful in microwave and magnetic recording devices because they have a small magnetic loss at high frequencies because of their insulating nature. High resistance and low power loss are two essential characteristics of magnetic materials. In addition, due to its ferromagnetic and low-loss dielectric properties, which include moderate magnetisation, strong coercivity, excellent chemical stability, and composition stability, it can be used in a variety of industries, including magnetic fluids, magnetic recording, and others alike [2].

1.3. Ferrites

Ferrite is a ceramic material composed of elements mixed with iron oxide because it is the primary component of ferrite, which makes ferrite to have useful properties. Naturally occurring ferrite is made from black iron oxide (Fe_3O_4 or Fe_2O_3). The electric and magnetic properties of ferrite materials allow their use in many applications, such as microwave components, high-frequency devices, and magnetic memory storage. Ferrites are mainly ionic and have extremely stable crystalline structures. Iron oxides of the type of spinel. It has the formula AB_2O_4 , where A is divalent transition cations like Fe^{2+} , Co^{2+} , Ni^{2+} , Zn^{2+} , etc. and B is Fe^{3+} having an ionic radius that approximately lies between 0.6 and 1 Å, which belongs to Fd-3m space group and O indicates the oxygen ion site. The general chemical formulation for spinel ferrite is $\text{A}^{+2}\text{Fe}^{+3}_2\text{O}_4$ [3,4].

1.4. Synthesis of Ferrite Nanoparticles

A set of chemical synthesis methods has just been developed in recent years. To prepare single-dispersion super magnetic nanoparticles depending on the size, composition, surface chemistry, and aggregation state. In particular, the practical methods were chemical co-precipitation, ceramics, sol-gel, and hydrothermal synthesis, and other methods [5]. Ferrite is an inexpensive material and its properties depend on the shape and size of nanoparticles, sintering temperature, method of preparation, and the type and quantity of ferrite-forming elements [6]. The properties of the prepared ferrite are controlled by controlling the redistribution of metal ions, and this is mainly responsible for the magnetic behavior of the prepared ferrite.

The nano ferrite can be obtained by controlling the number and accuracy of the pH, in addition to the concentration of the components of the preparation substance and the temperature of preparation, while maintaining the measurement of the concentration of chemical elements in the preparation of ferrite [7]. Due to some of the properties that ferrite possesses, it has been widely used as a substitute for many materials, like microwaves, magnetic recording, telecommunications, and sensors [8].

1.5. Nanotechnology and Nanomaterials

Nano refers to one billionth of the meter, while the nanometer (nm) to 10^{-9} m. The word Nano is derived from the Greek word (Nanos), which indicates dwarf nanotechnology was concerned with materials properly for the scale. Nanotechnology, in concert together nanoscience, has the ability to manipulate individual atoms and molecules. Nanomaterials are defined as materials with an average particle size of less than 100 nanometers that consist of nanoparticles. Distinctive characteristics like high surface area, low weight, and high strength. Actually, a nanometer is 100,000 times smaller than the diameter of a human hair, or one millionth of a millimeter. Physical and chemical characteristics are good in these materials nanomaterials characteristics are substantially relying upon their size, and shape. The properties of nanometric materials vary considerably from those of atoms as well as other materials on a non-nanoscale. In nanoscale, the characteristics of materials like electrical conductivity, mechanical strength are higher than those at the non-nano scale, and this is mainly due to their ultra-small properties [9,10].

1.5.1. Classification of Nanomaterials

Nanomaterials include a wide range of materials classified according to their chemical nature, where nanomaterials can be categorized into natural materials such as volcanic ash and industrial materials like smoke from fuel combustion. There is also another classification of nanomaterials depending on the dimensions of their particles that are subject to the nanoscale in the following categories [11,12].

1- Zero dimensional nanomaterials

They are materials that have nanometer - range dimensions in three directions. Most of these nanomaterials are shaped like spherical, with a diameter in the range (1-50) nm. Nanomaterials can be crystalline or amorphous, consisting of a single crystal or polycrystalline or in single crystalline states. These materials also exhibit various shapes and forms. They constitute atomic clusters and cluster assemblies [13,14].

2- One dimensional nanomaterials

1D nanomaterials have two dimensions in the nanometer range and one dimension outside the nanometre range. The materials are crystalline or amorphous in the single crystal or polycrystalline form and are either chemically pure or impure. Common forms of one-dimensional materials are in the form of nanotube, nanofiber, nanowire, and nanofilaments [15].

3- Two dimensional nanomaterials

2D nanomaterials have one dimension in nanometre range and two dimensions outside the nanometre range. This class of materials is usually amorphous or crystalline in nature. This materials include ultrathin films on a surface and multilayer material, disc, platelets, and nanoplates [16].

4- Three dimensional nanomaterials

In 3D nanomaterials, three dimensions are outside the nanometre scale. These materials are characterized by the presence of the three dimensions that are beyond (100 nanometers), while their internal dimensions are subject to the nanoscale through the presence of different materials that have nanoscale dimensions. These materials incorporate dispersions of nanoparticles, bulks, nanowires and nanotubes [17].

1.5.2. Production Methods of Nanomaterials

There are many ways to produce nanomaterials, depending on the synthesis and processing processes. For creating ultra-fine particles, these methods can be divided into two major ways.

1- Top-down approach

It is a method for producing nanomaterials from materials with large sized structures. This method starts with a palpable size of the material and gets smaller little by little until reaching the nanoscale. This is the way most of the small structures are mass produced. High- energy ball milling, etching, liquid phase techniques, and sputtering by top- down approach [18].

2- Bottom-up approach

This method is unlike the previous method of preparation, where the materials are prepared to be nanoparticles by the process of homogeneous or heterogeneous nucleation of molecules or atoms of liquid or gaseous substances. Most of the methods used in this process are chemical methods, and their work is based on assembling molecules or atoms into nanostructures by carefully controlling the chemical reactions that include the assembly of

nanoparticle micelle. Nucleation and growth are the two important processes in bottom-up approach. Nucleation is a process in which an aggregate of atoms is formed and is the first step of the phase transformation. The growth of nuclei takes place in the form of large crystalline particles. Method to produce Bottom-up material includes deposition techniques, chemical vapor deposition, solution-phase techniques and self-assembly techniques [19,20]. As shown in Figure 1.1.

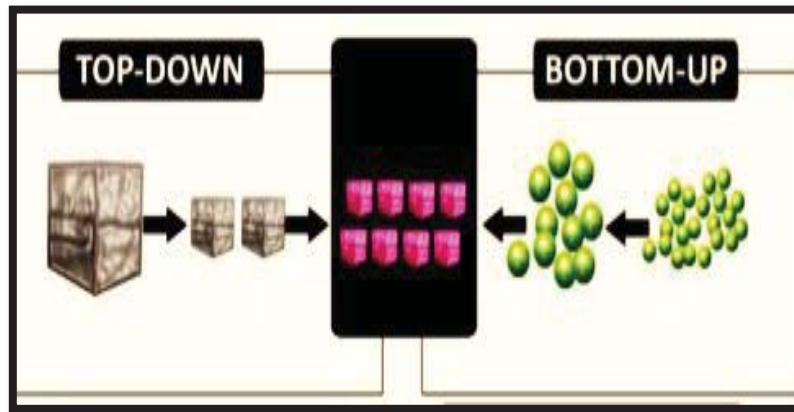


Figure 1.1: Schematic draw of bottom-up and top-down approach[19].

1.6. Applications of Ferrites

Nanomaterials are used in various fields due to their multidisciplinary nature, spinel ferrites are a common type of ceramic. In recent years, nano-ferrite become a very valuable material for a variety of applications. Bulk ferrites, such as Ni-Zn ferrite, are used as base materials for high frequency applications but cannot be used above 100MHz due to grain dimensions are all in micrometer scales and a material exhibits higher electrical conductivity, which causes eddy current losses [21]. To counter this problem, synthesizes the material with a greater level of electrical resistivity, which can be

accomplished by decrease the particle size of the material, causing a reduction in eddy current losses [22]. In addition, ferrite is employed in a wide range of tasks, including the lifting large iron objects and more complicated microwave, communications. radars, satellite communication, memory, and computer applications are additional examples. The most recent reason for the increase in interest in ferrite is the development of new miniature efficient power sources. Used in communications and computers are these power supplies because of their permeability high, saturation magnetization high, resistance high, and dielectric loss low because they directly help in noise suppression to the electronic circuits [23]. Ferrite particles with a spherical shape are desired for biomedical applications. Because spherical particles lack any prominent crystal planes, adhesion between the surfaces of nanoparticle spheres is unstable [24]. Ferro-fluids have also been proven to be the best form of magnetic nanoparticles for biomedical applications. The ferro-fluids were stable colloidal suspensions of the magnetic nanoparticles in a carrier liquid [25]. Furthermore, to stabilize a ferro-fluid, it is necessary that it be coated with suitable surfactants. These nanoparticles can be loaded with drugs and directed to specific parts of the body where a particularly diseased cell is located, thus avoiding interaction with healthy tissue. In spite of magnetic nanoparticles having several advantages in biomedical applications, they also have a number of drawbacks, including toxicity in biological systems, aggregation in solution, and limited surface accessibility [26]. As for the environmental applications, the presence of heavy metals in the wastewater is a menace to the ecosystem, where colored wastewater prevents solar radiation into the water. The release of colored wastewater could cause the photosynthetic response to slow down. As a result, removing colored dye from wastewater or degrading the dye to a less hazardous state before releasing it

into natural water resources is critical [27]. Magnetic nanoparticles are excellent dye adsorbents due to their high surface area capacity to become magnetized and demagnetized. These nanoparticles to the removal of impurities from water [28]. Therefore, the study of magnetic nanoparticles has become a fascinating subject of recent interest. In this research, we will focus on water treatment. In recent years, the supply of clean water for home and industrial use has been a major worry for both developed countries.

There are many people who do not have access to clean water [29]. Given the high population growth, it is certain that the amount of available water will decrease over time, negatively affecting the social and many countries' economies are developing. As a result, wastewater reuse could be a viable option in many nations [30]. Biodegradable organics, heavy metals, and pharmaceutical residues are all found in wastewater [31]. Nanoparticles were used in water treatment applications, where they focused on four basic areas: treatment, sensing, detection, and pollution control [32]. The most important technology used in water treatment is adsorption. Adsorption is an economical method for removing metal ions from wastewater. For good adsorption process, one must select the kind of an adsorbent that has a variety of properties like good adsorption compatibility, high surface area, high thermal conductivity, high mass diffusion, and thermal stability [33].

1.7. Previous Studies

Literature review is of the prime requirements and thus it was done to investigate the research and developmental activities that have been already carried out on ferrite nanoparticles.

(Kasapoglu et al., 2007), studied the structural properties of $\text{Ni}_x\text{Co}_{1-x}\text{Fe}_2\text{O}_4$ for values ($x=0-1$) prepared by hydrothermal method and sintered at (600 °C) for three hours. XRD and FTIR tests showed all prepared samples have spinel structure. From SEM test, showed morphological difference, the results indicate that the typical particle sizes are in the range (30-35) nm [34].

(Jing et al., 2007), studied the effect of the Gd ion on the structural and magnetic properties of (Li-Ni-ferrite), it have chemical formula $\text{LiNi}_{0.5}\text{Gd}_x\text{Fe}_{2-x}\text{O}_4$ for values ($x = 0.00$ to 0.08) prepared by rheological phase reaction method. The XRD analysis showed confined the single spinel phase was obtained in between ($x = 0.00$ to 0.04). All samples were spherical particles with an average size of about (100 nm), but agglomerated from AFM testing. By examining the magnetic properties, it can be seen that the saturation magnetization decreases with increase the Gd concentration [35].

(Costa et al., 2008), studied structural and magnetic properties for $\text{Ni}_{1-x}\text{Zn}_x\text{Fe}_2\text{O}_4$ for values ($x = 0.0 - 0.7$) prepared by combustion reaction method. The XRD test revealed that the crystal size increases with increasing zinc concentration, and the nanoparticle size is between (18 – 27) nm .The study of magnetic properties revealed that coercive field and saturation magnetization both increase with increase the zinc concentration [36].

(**Kambale et al., 2009**), studied the effect of Co^{2+} substitution on the structural and magnetic properties of $\text{Ni}_{1-x}\text{Co}_x\text{Fe}_2\text{O}_4$ for values ($x = 0.0$ to 0.8) prepared by standard ceramic technique and sintered at ($600\text{ }^\circ\text{C}$). The confirmation of single-phase formation and structural analysis were carried out by employing X-ray diffraction technique. According to the VSM test, with the increase of Co concentration the increase of saturation magnetization (M_s) and decreased coercive field (H_c) at higher Co^{2+} concentration ($x > 0.4$) [37].

(**Maqsood et al., 2011**), studied structural properties of $\text{Ni}_{1-x}\text{Co}_x\text{Fe}_2\text{O}_4$ for values ($x = 0.1$ to 0.5) prepared by chemical co-precipitation method. The XRD test showed that the nanoparticle size ranged between (15 - 33) nm [38].

(**Sivakumar et al., 2011**), Prepared nanoparticles NiFe_2O_4 by sol-gel method. Through testing, it was discovered that the NiFe_2O_4 compounds nanoparticles have a single-phase reverse spinel structure and are spherical in shape, with an average size of (8 nm). FTIR test for NiFe_2O_4 , show the tetrahedral and octahedral positions. Super-paramagnetic is observed with magnetic saturation (M_s) of (50.4emu/g) [39].

(**Sridhar et al., 2012**), studied effect of copper ion on structural properties for nickel ferrite have chemical formula of $\text{Ni}_{1-x}\text{Cu}_x\text{Fe}_2\text{O}_4$ for values ($x = 0, 0, 0.2, 0.4$ to 1.0) prepared by citrate gel technique. The X-ray pattern confirms that the spinel formation is monophasic and the crystal size of the ferrite nanoparticles is in the range (36 - 58) nm. The SEM analysis shows that the particle morphology is very similar. The sharpness of the particles is somewhat spherical with some agglomeration between the particles. EDS data

gives the elemental percentage and atomic percentage in the composition of the mixed nickel-copper ferrites, and shows the presence of nickel, copper, iron, and oxygen [40].

(Hankare et al., 2013), studied structural properties of $\text{Co}_{1-x}\text{Ni}_x\text{Fe}_2\text{O}_4$ for values ($x = 0.0$ to 1) prepared by the sol-gel technique. XRD test showed that all samples had one cubic spinel phase and the crystal size increases with increasing nickel content. The surface morphology and composition were also studied by SEM test and TEM test the nanostructure of the composite material ranges from (20-25) nm [41].

(Shrikant et al., 2013), studied the structural properties of $\text{MgNiFe}_2\text{O}_4$ prepared by sol-gel method, it having chemical formula of $\text{Mg}_{0.8}\text{Ni}_{0.2}\text{Fe}_2\text{O}_4$ and sintered at ($400\text{ }^\circ\text{C}$) for three hours. An XRD test showed that the average crystal particle size (28nm). From the (IR) test, the powders were characterized by spectroscopic analysis, and the composite material is ferrite [42].

(Azhagushanmugam, et al., 2013), studied the effect Zn ion on structural and magnetic properties of (Ni-Co ferrite) with the formula of $\text{Ni}_{0.8-x}\text{Co}_{0.2}\text{Zn}_x\text{Fe}_{2-x}\text{O}_4$ for values ($x = 0.2, 0.4$ and 0.6) prepared by chemical co-precipitation method. The samples XRD model showed that the cubic symmetry of the spinel structure was formed in a single phase. It has been found that the particle size decreases with increase the zinc concentration. A nanocrystalline state with an average particle size of about (17 nm) using

TEM. According to the VSM test, the coercive force (HC) and saturation magnetization (MS) decrease with the increase of Zn concentration [43].

(Mozaffari et al., 2014), studied the structural and magnetic properties of $\text{Ni}_{1-x}\text{Co}_x\text{Fe}_2\text{O}_4$ for values ($x= 0.1, 0.3$ to 0.9) prepared by sol-gel technique and sintered at ($500\text{ }^\circ\text{C}$) for three hours. The spinel structures in a single phase are confirmed by the XRD pattern. Additionally, according to FESEM images, the typical particle sizes were in the range from (70-160) nm. Magnetic measurements were made on the samples, and the results showed that as x increases, saturation magnetization and coercive forces decrease due to changes in magnetisms anisotropy [44].

(Yattinahalli et al., 2014), studied the structural properties of NiFe_2O_4 prepared by the chemical co-precipitation method. The XRD test showed that the particles have a cubic spinel structure and a nanoparticle size of (44-62) nm [45].

(Tirupanyam et al., 2015), studied the structural and magnetic properties of $\text{Mn}_x\text{Ni}_{1-x}\text{Fe}_2\text{O}_4$ for values ($x = 0.5, 0.6, 0.7$) prepared by co-precipitation method and sintered at ($800\text{ }^\circ\text{C}$). The XRD test showed the antiferromagnetic $\alpha\text{-Fe}_2\text{O}_3$ phase along with the magnetic spinel phase. They observed the crystal size increase with an increasing concentration of Mn^{2+} . From the VSM test, the saturation magnetization (M_S) decreases, while coercive strength (H_C) increases with the increasing of Mn^{2+} concentration [46].

(Rosnan et al., 2016), studied the effect of Mg substitution on the structural and magnetic properties for $\text{Co}_{0.5}\text{Ni}_{0.5-x}\text{Mg}_x\text{Fe}_2\text{O}_4$ prepared by coprecipitation method. The XRD test showed that the samples had a monophasic spinel structure with a crystal size of between (32-36) nm. FTIR indicates the formation of ferrite spinel functional groups by further substitution of Mg^{2+} . Images from a FESEM test display homogeneous samples with evenly spaced grains. It can be seen from the results of the VSM test samples that are prepared at room temperature that maximum magnetization and coercive force are increasing, respectively [47].

(R Sepahvandi et al., 2017), $\text{Co}_{1-x}\text{Mg}_x\text{Fe}_2\text{O}_4$ nanoparticles with x values (0, 0.5, and 1) synthesized using a microwave-assisted combustion method and subsequent heat treatment. According to the Scherrer formula, the average crystal size of the composite samples was about (32 nm). The saturation magnets (Ms) for the samples with x-values of 0, 0.5, and 1 were 59, 27, and 28 emu/g, respectively. The results showed that the magnetization and remanent magnetization directly changed with the increasing of Cobalt concentration [48].

(Anupama et al., 2018), studied effect of Zn substitution on the structural and magnetic properties of $\text{Ni}_{1-x}\text{Zn}_x\text{Fe}_2\text{O}_4$ prepared by sol-gel combustion technique. The cubic spinel is confirmed by the XRD pattern without the formation of any impurity phases. SEM and TEM micrographs show the agglomerated particles to be in the nano range in terms of size. According to measurements with VSM, pure Ni ferrites exhibit soft magnetic behavior.

Additionally, the Zn ion was substituted for and its concentration was increased in Ni ferrites to suppress their ferromagnetic behavior [49].

(Ateia et al., 2018), studied effect of Ni ion on the structural and magnetic characteristics of Co ferrite nanoparticles for values ($x = 0.0$ to 1.0) prepared by sol-gel technique and sintered at ($600\text{ }^{\circ}\text{C}$) for 4 h. The size of the crystallites ranged between (24-27) nm. When nickel is added, there are changes in the lattice modulus, roughness, surface area, and porosity volume. From magnetic tests, the magnetic behavior revealed an increase in coercivity (H_c) [50].

(Mohamed et al., 2019), $\text{Co}_x\text{Zn}_{1-x}\text{Fe}_2\text{O}_4$ nanoparticles were prepared by precipitation and hydrothermal methods, and the effect of the Co ion on their structural and magnetic properties had been studied. The XRD pattern confirms a single-phase spinel structure and the calculated grain sizes for samples ranges from (8.3-11.4) nm. Theoretical and measured elemental stoichiometry were found to be in good agreement by the EDX test, and SEM and TEM tests confirmed the sphere-like morphology of the particles with diameters of (10 nm). The magnetic phase changes from paramagnetic to superparamagnetic as the cobalt doping level is increased [51].

(Ajeesha et al., 2021), studied the magnetic and structural properties of $\text{Mg}_{1-x}\text{Ni}_x\text{Fe}_2\text{O}_4$ for ($x=0.0-1$) ferrite nanoparticles prepared by the chemical co-precipitation technique . Tests using XRD and TEM revealed that the cubic spinel phase belongs to the $Fd-3m$ space group and that the average crystal size (D) is between (20-30) nm. Measurements of the VSM point to ferromagnetism [52].

(Arifuzzaman et al., 2021), studied the impact of the Cu ion on the structural and magnetic characteristics of ferrite nanoparticles, which have a chemical formula of $\text{Ni}_{0.7-x}\text{Cu}_x\text{Cd}_{0.3}\text{Fe}_2\text{O}_4$ which were made using the sol-gel method and heated at (700 °C). According to XRD, the samples as-prepared formed the cubic spinel phase, with the materials average crystallite size between (18 -29) nm. The nanocrystalline nature of the examined samples was revealed by TEM and FESEM. The ferromagnetic character is demonstrated through the hysteresis loop VSM tests for samples prepared at room temperature, and the saturation magnetization is observed to decrease with Cu substitution [53].

(Ahmed et al., 2022), studied structural and magnetic properties for $\text{Ni}_{x-1}\text{Zn}_x\text{Fe}_2\text{O}_4$ for values ($0 \leq x \leq 1$) prepared by co-precipitation method. The XRD test revealed that the crystal size increases with increasing zinc concentration, and the nanoparticle size is between (16.56 – 12.95) nm. FTIR spectroscopy showed that replacement with Zn up to $x = 0.5$ in $\text{Ni}_{x-1}\text{Zn}_x\text{Fe}_2\text{O}_4$ nanocrystals led to the migration of iron ions from tetrahedral to octahedral sites. The study of magnetic properties revealed with the increase of Zn^{2+} concentration the increase of saturation magnetization (Ms) and decrease coercive field (Hc) [54].

1.8. Study Aim

- 1- The preparation of magnetic nanoparticles from nickel-cobalt ferrite ($\text{Ni}_{1-x}\text{Co}_x\text{Fe}_2\text{O}_4$) and nickel-magnesium ferrite ($\text{Ni}_{1-x}\text{Mg}_x\text{Fe}_2\text{O}_4$) by using the chemical co-precipitation thermal method for ($x=0.0, 0.1, 0.3, 0.5, 0.7$).
- 2- Studying the structural and magnetic properties using XRD, EDX, SEM, FTIR, and VSM. Then choosing the best two samples of prepared magnetic nanoparticles from each mixture based on their structural and magnetic properties for use in the application of water treatment.
- 3- A graphene oxide derivative with 2(N-morpholino ethanesulfonic acid) was synthesized and characterized using FTIR, ^1H NMR, XRD, and TEM.
- 4- The GO- 2(N-morpholino ethanesulfonic acid) was used to prepare novel magnetic adsorbents by mixing with the best four ferrites. These nanocomposites were characterized using XRD, TEM, and VSM.
- 5- Studying the effects of various factors like contact time, pH, dosage, and temperature, and knowing out which of the four magnetic adsorbents is best to remove (lead and cadmium ions) from aqueous solutions.
- 6- Studying the adsorption kinetic from through the use of first-order and second-order models, and the determination of the best model for the adsorption process and adsorption processes by using Langmuir, Freundlich, and Temkin isotherms and determining which equation best describes the adsorption system.